ISBN: 978-3-95450-262-2 ISSN: 2673-5350 doi: 10.18429/JACoW-IBIC2025-WEPCO06

PERFORMANCE ANALYSIS OF RF ANALOG FRONTEND FOR DIAMOND–II ELECTRON BEAM POSITION MONITORS

H. I. Malik*, M. G. Abbott, L. Bobb, M. Zeeshan
Diamond Light Source, Oxfordshire, United Kingdom

Abstract

Diamond-II is a major upgrade to the current synchrotron facility, Diamond Light Source. The low emittance electron beam requires more stable, low drift beam position monitor electronics which are also essential for the Fast Orbit FeedBack system. This paper presents simulated results of the analog frontend for the electron beam position monitors. This work aims to deliver an analog frontend with stable gain and high linearity that meets the dynamic range and noise figure requirements effectively to capture beam positions for single and multi-bunch operation. Performance evaluations have been conducted using the SystemVue simulation suite.

INTRODUCTION

Diamond Light Source currently operates using a 3 GeV electron beam for the generation of high power X-rays for beamline experiments. A major upgrade is on the way to upgrade the current machine to a fourth generation synchrotron where the electron beam energy will be increased from 3.0 to 3.5 GeV. This will provide scientists with increased brightness and coherence for enhanced experimentation and analytic capabilities. Table 1 summarizes the system requirements for the Electron Beam Position Monitors (EBPM) for Diamond–II (D-II) [1–3].

Table 1: Diamond-II EBPM Requirements

Parameter	Diamond-II
Number of EBPMs	252 (11/12 per cell)
Geometric factor k	7.3 mm
Short-term motion (<1 s)	
Commissioning (0.3 mA)	$<130\,\text{nm}/\sqrt{\text{Hz}}$
User beam (300 mA)	$<2\,\text{nm}/\sqrt{\text{Hz}}$
Long-term motion (<1wk)	<1 µm pk-pk

Figure 1 presents the system level diagram for the complete EBPM electronics. In the storage ring the longitudinal placement of the analog frontend (AFE) on the girder is determined by the position of the button assemblies, and vertically they will be placed at the base of the girder to receive minimal radiation. Each girder has 6-8 analog frontends as shown in Fig. 1. A latest inclusion in the design architecture is the Pilot Tone Distributor module (PTD). A PTD module is responsible for receiving the pilot tone from the Control and Instrumentation Area (CIA) and distributing it to Pilot Tone Injectors (PTI), where the power out of the pilot tone distributor is remotely configurable depending on operational mode requirements.

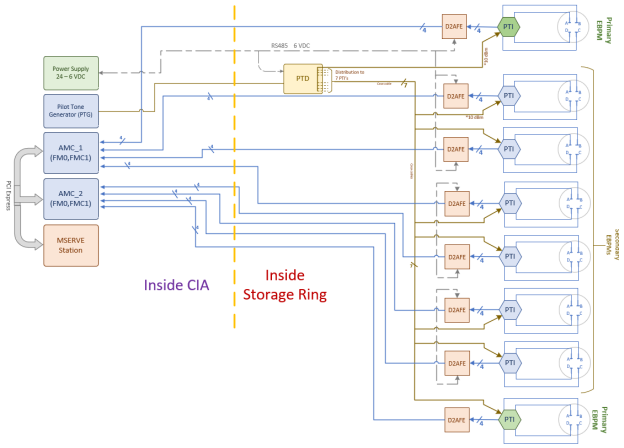

Figure 1: System level diagram of the EBPM architecture.

D-II ANALOG FRONTEND

The initial work on the D-II analog frontend (D2AFE) is described in [2]. Figure 2 presents the proposed RF chain. The input signal is fed from to the low pass filter (LPF) at 500 MHz, followed by an LC bandpass filter and a digital tunable step attenuator. The first amplifier is a Low Noise amplifier (LNA) with a noise figure of 0.45 name and gain of 24 name, where it contributes mainly towards defining the overall noise figure of the RF chain. The amplifier is followed by a LPF for harmonic suppression and a step attenuator for amplitude control.

The second stage amplifier is a gain block amplifier with higher linearity and a linear gain of 20 dB. A second LC bandpass filter is used for extra filtering and signal conditioning before providing the signal to a 0.5 dB directional coupler. The coupler couples the signal to a log detector for power estimation of the RF signal. An onboard micro controller based analog to digital converter is then used to digitize the detected RF power.

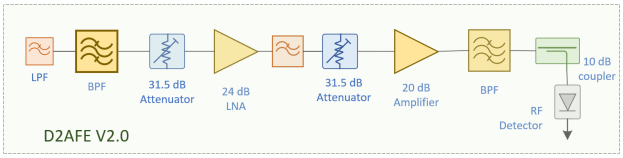

Figure 2: Proposed analog frontend RF chain.

* hasan.malik@diamond.ac.uk

ISBN: 978-3-95450-262-2 ISSN: 2673-5350 doi: 10.18429/JACoW-IBIC2025-WEPCO06

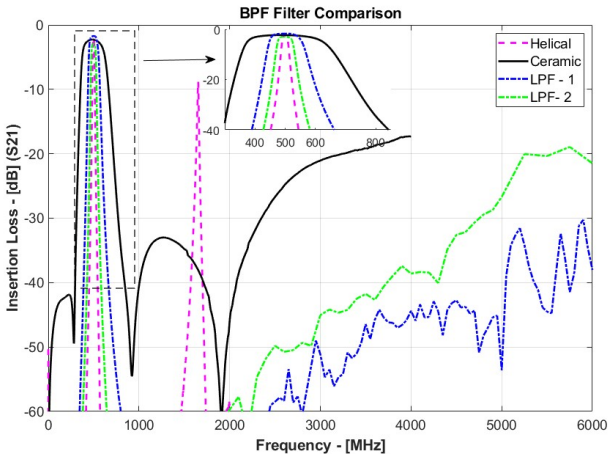

Figure 3: Comparison of filtering methodologies.

LC Filters

A major design change in the D2AFE was carried out to replace the existing helical filters with pre-tuned LC filters. The helical filters were replaced due to their manual tuning screws for frequency adjustment. It was not practically feasible to tune 24 screws for a single board. Thus, a pre-tuned filter bypasses this production limitation. A comparison was drawn among the different filter candidates available. Figure 3 shows the insertion loss of commercially available off the shelf ceramic, LC and helical filters. The helical filter has the best narrowband response and sharp roll-off at 500 MHz, but with a harmonic resonance at 1.65 GHz. The ceramic filter offers the widest bandwidth at 500 MHz. The plot also presents the passbands for two pre-tuned LC filters centered at 500 MHz. The pre-tuned LC filters offer better high frequency harmonic suppression. SAW filters also offer excellent roll offs and harmonic rejection but were not considered due to their temperature dependent frequency response [4]. Additionally, it can be seen in Fig. 3 that the selected LC-1 filter offers better rejection of more than 30 dB up to 6 GHz.

Band Limited Gain Block Amplifier

In order to improve the linearity and harmonic behavior of the RF chain, a gain block amplifier was used as a second stage amplifier. The selected device offers a gain of 20 dB with a band limited operation up to 500 MHz.

Removal of Pilot Tone Injector

An external PTI module closer to the button assemblies on the girder will be used, therefore PTI circuitry was removed from the analog frontend board. This includes the removal of the 10.5 dB coupler in the RF chain along with the removal of the tunable attenuators for the pilot tone power control. This removal of PTI from the D2AFE brings the board stackup from a 6 to 4 layer board, reducing the complexity and production cost.

SYSTEMVUE SIMULATIONS

In order to validate and analyze the effect of the proposed changes on the RF properties of the board, the RF chain was modeled using the Keysight SystemVue software [5]. The RF chain was considered along with the passive components ahead of the D2AFE. This included the PTI and a hand formable coaxial cable (sucoform-141) between the button assemblies and the PTI. An RF cable (LMR-240) was included as a lossy component between PTI and D2AFE. The simulations were performed to analyze gain, noise figure, linearity and dynamic range for the RF chains.

Figure 4 presents the simulation results for gain and dynamic range of the proposed RF chain, considering input signal over a power range of -70 to 0 dBm. This power range corresponds to the maximum and minimum RF signal induced at the BPM buttons for beam commissioning and full current operation. The gain contributions of individual components scale the input signal as shown in Fig. 4. A major attenuator switching happens at the first step attenuator to avoid any saturation of the first LNA amplifier. The second stage attenuator also changes attenuation states as the input signal increases further to limit the RF power fed to the gain block amplifier.

The simulation shows the output RF power range of -45 to 4 dBm for an input RF power of -70 to 0 dBm. The RF chains use 0.5 dB attenuation steps with 6 bit resolution, offering a maximum attenuation range of 31.5 dB. In order to evaluate the noise floor offered by the proposed RF chain, SystemVue noise simulations were performed using non-linear data for each component.

Figure 5 presents the cumulative noise figure for the RF chain. It can be seen that a major contribution towards noise figure comes from the initial passive RF components in the chain. The noise figure rises to a constant of 7.8 dB as the signal propagates through the RF chain. The bandwidth of the LC BPF filters is 20 MHz centered around 500 MHz and limits the analog noise of the RF chain. The noise floor with minimal attenuation level for the RF chain was simulated to be −94 dBm, which is sufficiently below the system requirements of −71 dBm.

PROTOTYPE ANALOG FRONTEND BOARD

A D2AFE board was modeled using the Cadence design tool [6] and is currently in fabrication as shown in Fig. 6. In order to shield the electronic board from humidity effects, the board will be housed in a milled enclosure. This also provides better RF shielding from external ambient RF noise. Special considerations were taken into account to improve the noise immunity of the RF chains from the digital noise created by the on-board microcontroller. The power regulation section in the board layout was improved by providing better heat sinking paths for the linear dropout regulators via exposed soldermask regions on the bottom side of the board. This provides a heat conduction path to the metallic chassis.

ISBN: 978-3-95450-262-2 ISSN: 2673-5350 doi: 10.18429/JACoW-IBIC2025-WEPCO06

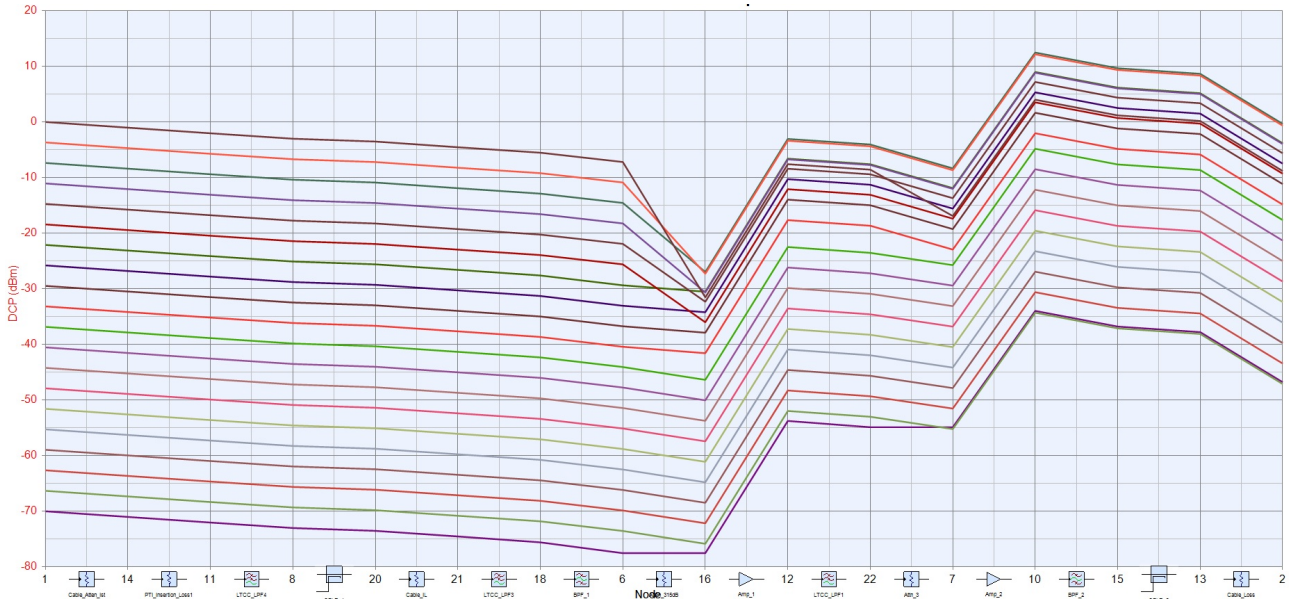

Figure 4: Desired Channel Power (DCP) of D2AFE RF chain to cover -70 to 0 dBm input power range.

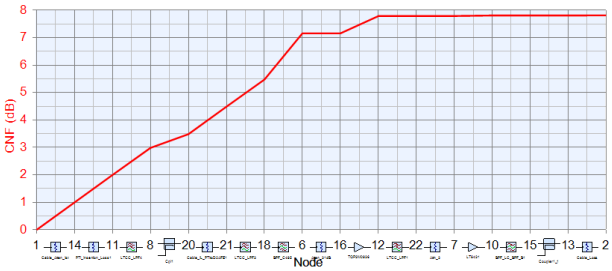

Figure 5: Cumulative noise figure for RF chain.

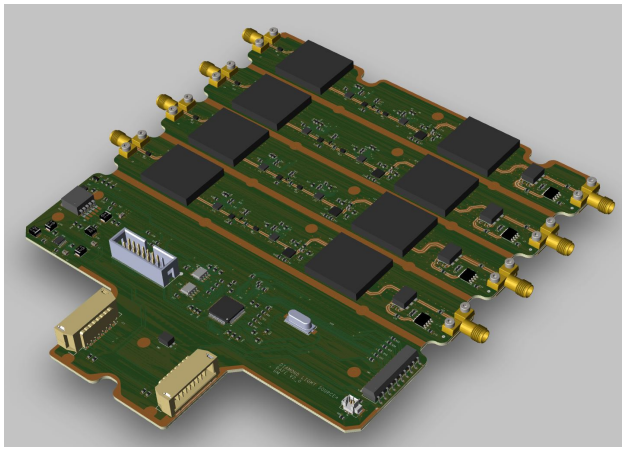

Figure 6: Modelled D2AFE board PCB layout.

CONCLUSION

This paper discusses progress in the development of an analog frontend for the Diamond–II EBPM electronics. Improvements and enhancements in the design include the replacement of helical filters with pre-tuned LC filters, the use of band limited RF gain block amplifiers, the removal of the on-board PTI circuitry and an enhanced layout considerations. SystemVue simulations were performed to analyze the effect of these proposed changes. Results show that the frontend is able to achieve a board dynamic range from –71 to 0 dBm, required to support beam commissioning and full current operation of 300 mA. A board layout has been modeled and sent for fabrication.

REFERENCES

[1] R. P. Walker *et al.*, *Diamond-II Technical Design Report*, Diamond Light Source Ltd., Oxfordshire, UK, Tech. Rep., 2022, https://www.diamond.ac.uk/Home/News/LatestNews/2022/14-10-22.html

[2] L. T. Stant *et al.*, "Diamond-II Electron Beam Position Monitor Development", in *Proc. IBIC'22*, Kraków, Poland, Sep. 2022, pp. 168–172. doi:10.18429/JACoW-IBIC2022-MO3C2

[3] A. F. D. Morgan, "Technological Review of Beam Position Button Design and Manufacture", in *Proc. IBIC'19*, Malmö, Sweden, Sep. 2019, pp. 448–452. doi:10.18429/JACoW-IBIC2019-WEAO01

[4] J. Zhang *et. al.*, "High temperature effects on surface acoustic wave strain sensor", in *Sens. Actuators A: Phys.*, vol. 338, May 2022. doi:10.1016/j.sna.2022.113464

[5] Pathwave SystemVue Design, 2022, www.keysight.com/gb/en/products/software/pathwave-design-software/pathwave-system-design-software.html

[6] Cadence: Orcad X Platform, 2022, www.cadence.com/en_US/home/tools/pcb-design-and-analysis/orcad.html